

dances) was capable of diffusing into the regolith and condensing as pore ice within the top few meters in these regions of stability. The timescale of condensation of ice from atmospheric water was found to be comparable to that of the evolution of the martian orbit, indicating the need to include past orbital changes in the prediction of the present distribution of ground ice. In the present work we include the past orbital evolution of Mars and examine the changes in ice stability as well as the condensation, sublimation, and diffusion of atmospheric water in an exchange with the regolith.

The martian obliquity has undergone significant oscillations in its recent past. During periods of high obliquity the solar energy would have been distributed such that the equatorial and mid-latitude regions would have been colder than at present and the polar regions would have been warmer. Warmer polar regions would result in the sublimation of more polar cap water into the atmosphere and thus higher atmospheric water abundances. This combination of effects would have resulted in ground ice being stable globally. During periods of low obliquity the opposite would have occurred, where the equatorial and midlatitude regions were warmer and the polar regions were colder, resulting in less atmospheric water and ground-ice stability only in the polar regions.

The results of our modeling of the regolith thermal behavior and the molecular diffusion of water vapor within the regolith and in exchange with the atmosphere have shown significant quantities of ground ice can form at all latitudes within the top 50 cm to 1 m of the regolith during periods of high obliquity. The amount of ice that forms can be as much as the regolith pores can hold. During low obliquity most or all of this ice sublimates and diffuses away. Below this depth a longer-term stability is observed at some latitudes where ice steadily increases in concentration regardless of the orbital oscillations that occur.

These changes in the pattern of ice stability may affect the surface morphology at all latitudes. Periodic saturation and dessication of the regolith may produce some type of frost-heave-related features such as solifluction or stone sorting. The presence of ice in conjunction with seasonal thermal cycles may produce small-scale (a few meters) ice-wedge polygons or other forms of segregated ice.

## N94-33219

529-91 ABS ONI  
 2-3  
 MINERALOGICAL DIVERSITY (SPECTRAL REFLECTANCE AND MÖSSBAUER DATA) IN COMPOSITIONALLY SIMILAR IMPACT MELT ROCKS FROM MANICOUAGAN CRATER, CANADA. R. V. Morris<sup>1</sup>, J. F. Bell III<sup>2</sup>, D. C. Golden<sup>1</sup>, and H. V. Lauer Jr.<sup>3</sup>, <sup>1</sup>Code SN4, NASA Johnson Space Center, Houston TX 77058, USA, <sup>2</sup>NASA Ames Research Center, Moffett Field CA 94035, USA, <sup>3</sup>Lockheed ESC, Houston TX 77058.

**Introduction:** Meteoritic impacts under oxidizing surface conditions occur on both Earth and Mars. Oxidative alteration of impact melt sheets is reported at several terrestrial impact structures including Manicouagan [1], West Clearwater Lake [2], and the Ries Basin [3,4]. A number of studies [e.g., 5-7] have advocated that a significant fraction of martian soil may consist of erosional products of oxidatively altered impact melt sheets. If so, the signature of the Fe-bearing mineralogies formed by the process may be present in visible and near-IR reflectivity data for the martian surface.

What mineral assemblages form in impact melt sheets produced under oxidizing conditions and what are their spectral signatures? We report here spectral and Mössbauer data for 19 powder samples of impact melt rock from Manicouagan Crater. Experimental procedures are discussed elsewhere [8,9].

**Results and Discussion:** Previous chemical and petrographic studies. One of the important conclusions of chemical studies of Manicouagan impact melt rocks [1] is that there is no significant difference in the bulk composition with respect to either vertical or horizontal sampling of the impact melt sheet (230 m thick and 55 km

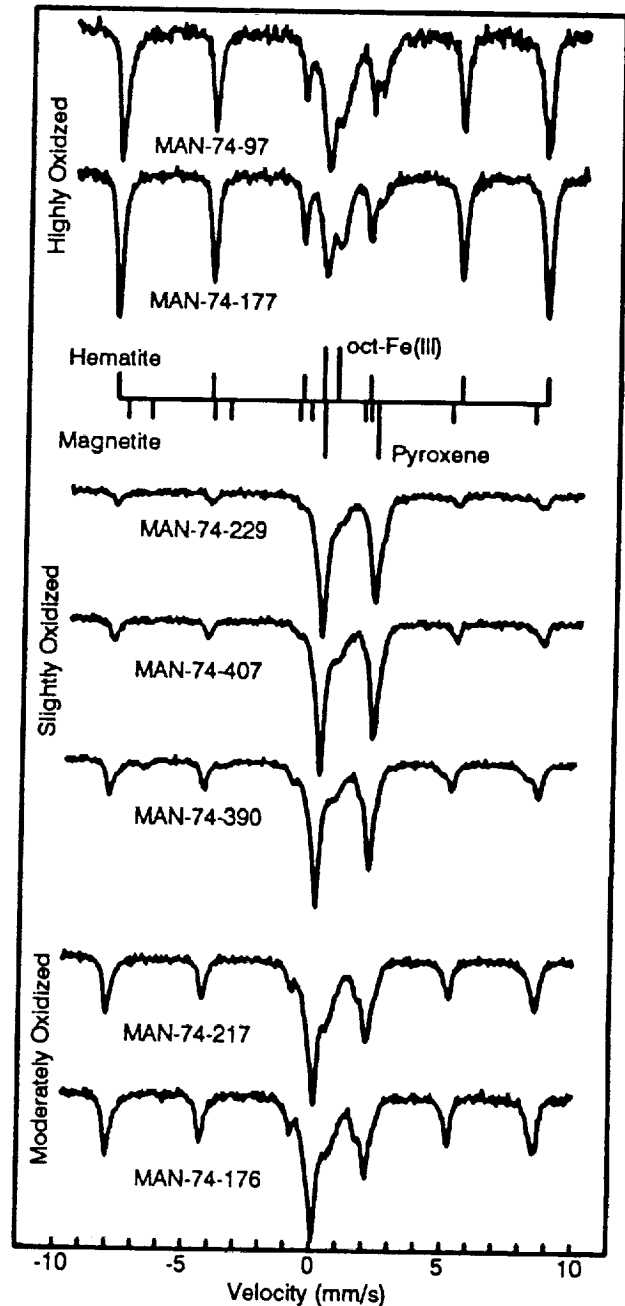


Fig. 1.

wide). Although chemical compositions are similar, the oxidation state of Fe is highly variable:  $FeO/(FeO + Fe_2O_3)$  varies from 0.142 to 0.639. However, there is still no significant difference in chemical composition when the samples are grouped according to  $FeO/(FeO + Fe_2O_3)$ . The 12 samples with the lowest values have the same average composition as the 12 samples with the highest values. All samples are at least somewhat oxidized as [1] estimate a prealteration value of 0.77.

The mineralogy of the impact melt rocks [1] includes plagioclase, sanidine, Ca-rich pyroxene, pigeonite (in various stages of inversion to hypersthene), quartz, titaniferous magnetite, and apatite. Approximate pyroxene compositions are  $Wo_{40}En_{42}Fs_{18}$  and  $Wo_4En_{53}Fs_{43}$ . Alteration (oxidation and/or hydration) products of glass, mafic minerals (mainly olivine and Ca-poor pyroxene), and oxides are smectite, hematite, and possibly hydrous ferric oxides [1]. The alteration is thought to have occurred shortly after the impact when oxidizing vapors and/or solutions (probably of external origin) reacted with the impact melt, which was below its solidus temperature but still relatively hot.

**Mössbauer and Reflectivity Spectra: Highly oxidized samples ( $FeO/(FeO+Fe_2O_3) < 0.250$ ).** Representative Mössbauer and reflectivity spectra are shown in Figs. 1 and 2. The Mössbauer spectra are dominated by a hematite ( $\alpha-Fe_2O_3$ ) sextet; the asymmetry of the lines implies impurities (probably Ti) are present. There is no evidence for a goethite ( $\alpha-FeOOH$ ) sextet. A doublet resulting from octahedrally coordinated ferric iron and a small doublet resulting from ferrous iron in pyroxene are also present. The origin of the ferric doublet cannot be uniquely assigned at present. It could result from pseudobrookite solid solutions (from ilmenite oxidation) or from ferric iron in a silicate phase such as pyroxene or smectite. Nanophase ferric oxides and lepidocrocite ( $\gamma-FeOOH$ ) are unlikely because, respectively, the doublet was not removed by extraction with DCB and not magnetically split by 16 K. The reflectivity spectra are dominated by the signature of hematite (band minimum or plateau center near 840 nm, relative reflectivity maximum near 750 nm, and inflections near 620 and 520 nm [e.g., 10]).

*What is the origin of the hematite?* The Mössbauer and reflectivity spectra of MAN-74-177 are virtually identical to those published by [11] for Hawaiiitic tephra sample HWMK 11. As discussed by [11], this sample is completely oxidized (presumably by heating to a high temperature) and contains hematite grains with highly variable Ti contents. The larger hematite grains are Ti rich and were attributed to thermal oxidation and phase separation of precursor Ti-magnetites. Fine hematite grains are distributed throughout the glass matrix, are Ti poor, and were formed from exclusion of silicate phases (including glass) during thermal oxidation. Phinney et al. [2] describe a similar situation for the reddish impact melt rocks from West Clearwater Lake. Straub et al. [12] report the formation of nanophase hematite during the thermal decomposition of pyroxene. Thus, it is reasonable to conclude that hematite formation in the highly oxidized Manicouagan impact melt samples preceeded by thermally induced magnetite oxidation and silicate decomposition.

*Slightly oxidized samples ( $FeO/(FeO+Fe_2O_3) > 0.500$ ).* Hematite is still present but in significantly lesser amounts than in the heavily oxidized samples (Figs. 1 and 2). Magnetite is present in MAN-74-390. The ferrous doublet from pyroxene is the dominant feature in the Mössbauer spectra. The two-band signature typical of ferrous iron in orthopyroxene and type-B clinopyroxene [13] is

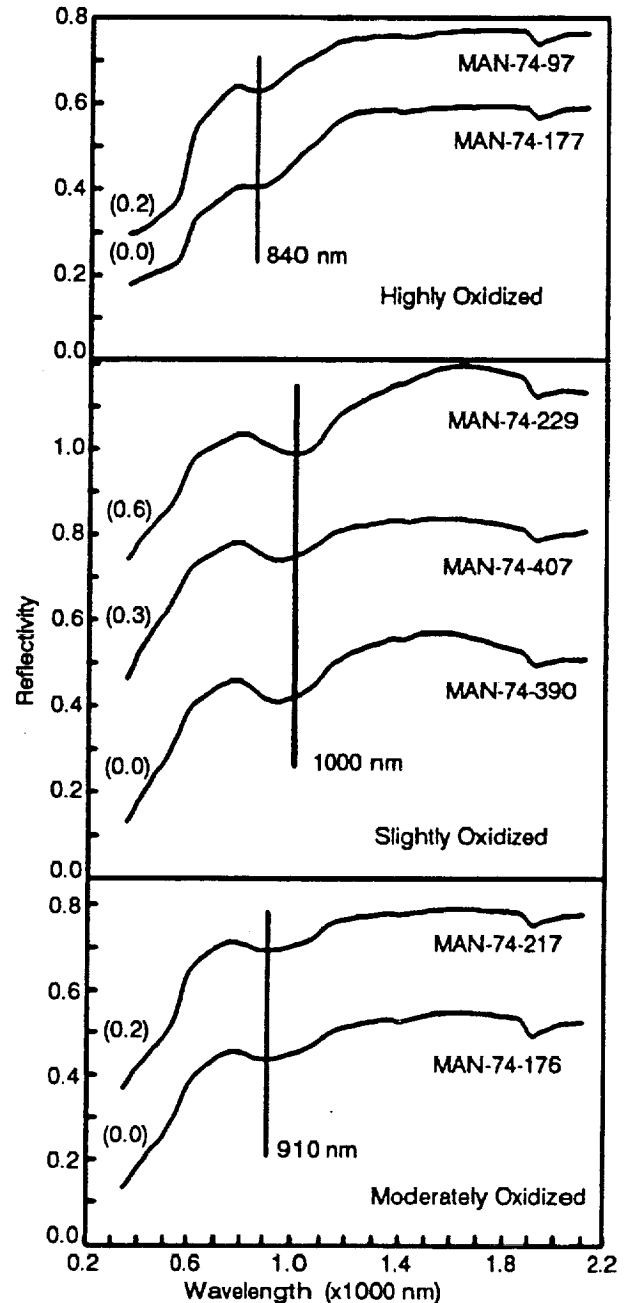


Fig. 2.

clearly evident in the reflectivity spectra. The position of the first band is well defined and varies from ~940 nm to 1000 nm, which implies more than one pyroxene is present. The positions are consistent with the high- and low-Ca pyroxenes [13] observed petrographically [1]. Positions of the second bands are not definable because they are partially obscured by  $H_2O$  bands near 1900 nm and our data do not extend to long enough wavelength.

*Moderately oxidized samples  $0.500 > (FeO/(FeO+Fe_2O_3)) > 0.250$ .* Mössbauer and reflectivity spectra for two samples having

530 91 405.6

intermediate values of  $\text{FeO}/(\text{FeO} + \text{Fe}_2\text{O}_3)$  are shown in Figs. 1 and 2. Their Mössbauer spectra show more comparable amounts of hematite and pyroxene than the heavily and slightly oxidized samples. The reflectivity data for both have a band minimum near 910 nm, which could result from (1) a composite of hematite (840–870-nm) and pyroxene (940-nm) bands; (2) a different pyroxene characterized by a 910-nm band; (3) a composite band derived from a pyroxene ferrous band and a pyroxene ferrous-ferric charge transfer band; and (4) another ferric mineral (e.g., goethite) having a band in this region. Alternative (4) is excluded by the Mössbauer data specifically for the case of goethite. None of the other alternatives can be excluded. However, a pyroxene 910-nm band usually implies a second band near 1800 nm [13], which we would probably observe, and [12] did not observe ferrous-ferric charge transfer transitions in two-band pyroxenes they subjected to thermal oxidation in air. Thus, there is some evidence to favor the interpretation involving composite hematite-pyroxene bands. This is particularly the case for MAN-74-217, where the 750-nm relative reflectivity maximum and 620- and 520-nm inflections are evidence for a strong spectral contribution from hematite.

#### Implications for Interpretation of Martian Spectral Data:

Visible and near-IR martian bright-region spectral data (400 to ~2000 nm) returned from groundbased telescopes and the Phobos-2 encounter are characterized by a shallow band minimum in the near-IR whose position varies between approximately 850 and 1000 nm [14,15]. It is reasonable to assign these endmember band positions to hematite and pyroxene respectively [8,14,15]. Assignment of band positions near 910 nm is more equivocal. Murchie et al. and Geissler et al. [14,16] favor another ferric phase (like goethite) as the interpretation for Phobos-2 bands in the region of 910 nm, although they do not exclude composite hematite-pyroxene bands. The results of this study show for naturally occurring materials that composite hematite-pyroxene bands have minima in the 910-nm region. Thus, many of the anomalous Phobos-2 spectra can be explained by assemblages whose endmembers (hematite and pyroxene) are accepted to be present on Mars. Furthermore, our results show that a mineralogically diverse suite of rocks can be generated at essentially constant composition, which implies that variations in martian surface mineralogy do not necessarily imply variations in chemical composition.

**References:** [1] Floran et al. (1978) *JGR*, 83, 2737. [2] Phinney et al. (1978) *LPS IX*, 2659. [3] Pohl et al. (1977) *Impact and Explosion Cratering*, 343. [4] Newsom et al. (1986) *Proc. LPS 17th*, in *JGR*, 91, E239. [5] Newsom (1980) *Icarus*, 44, 207. [6] Kieffer and Simonds (1980) *Rev. Geophys. Space Phys.*, 18, 143. [7] Allen et al. (1982) *JGR*, 87, 10083. [8] Morris et al. (1989) *JGR*, 94, 2760. [9] Morris et al. (1993) *GCA*, in press. [10] Morris et al. (1985) *JGR*, 90, 3126 [11] Golden et al. (1993) *JGR*, 98, 3401. [12] Straub et al. (1991) *JGR*, 96, 18819. [13] Cloutis and Gaffey (1991) *JGR*, 96, 22809. [14] Murchie et al. (1993) *Icarus*, in press. [15] Bell et al. (1990) *JGR*, 95, 14447. [16] Geissler et al. (1993) *Icarus*, in press.

**MARTIAN SPECTRAL UNITS DERIVED FROM ISM IMAGING SPECTROMETER DATA.** S. Murchie<sup>1</sup>, J. Mustard<sup>2</sup>, and R. Saylor<sup>3</sup>, <sup>1</sup>Lunar and Planetary Institute, Houston TX 77058, USA, <sup>2</sup>Brown University, Providence RI 02912, USA, <sup>3</sup>Western Kentucky University, Bowling Green KY 42101, USA.

**Introduction:** Based on results of the Viking mission, the soil layer of Mars has been thought to be fairly homogeneous and to consist of a mixture of as few as two components, a "dark gray" basaltic material and a "bright red" altered material [1,2]. However, near-infrared reflectance spectra measured recently both telescopically and from spacecraft indicate compositional heterogeneity beyond what can be explained by just two components [3,4]. In particular, data from the ISM imaging spectrometer [4,5], which observed much of the equatorial region at a spatial resolution of ~22 km, indicate spatial differences in the presence and abundance of Fe-containing phases, hydroxylated silicates, and H<sub>2</sub>O [4,6–8]. We have used the ISM data to define, characterize, and map soil "units" based on their spectral properties. The spatial distributions of these "units" were compared to morphologic, visible color, and thermal inertia features recognized in Viking data.

**Analysis:** We investigated ISM data "windows" that cover eastern Tharsis, Valles Marineris, Arabia, Syrtis Major, Isidis, and Amenthes. These areas contain examples of most of the variations in color, reflectance, and thermal inertia recognized in Viking data [2]. The windows were registered with the digital topographic map of Mars using spacecraft pointing information and correlation of topographic relief features with variations in depth of the 2.0- $\mu\text{m}$  atmospheric CO<sub>2</sub> absorption. The ISM data were reduced to a suite of "parameter" images that describe key sources of spectral variability, including reflectance, strength of a narrow absorption at 2.2  $\mu\text{m}$  attributed to metal-OH, depth of the 3.0- $\mu\text{m}$  H<sub>2</sub>O absorption, depth of the broad 2- $\mu\text{m}$  absorption attributed to Fe in pyroxene, and NIR spectral slope. Representative spectra were extracted for regions displaying different spectral characteristics to validate these differences and to characterize the shape and position of the 1- $\mu\text{m}$  and 2- $\mu\text{m}$  absorptions due to ferric and ferrous iron.

The parameterized ISM data were then classified using principal components analysis. Three principal components were found capable of accounting for most of the observed variations in NIR spectral properties. Spatial variations in the contributions or "loadings" of the principal components define coherent regions of soils having distinctly different spectral properties.

**Results:** The observed martian soils can be divided into broad groupings (Table 1) based on systematic, spatially coherent differences in their spectral attributes. The two largest groupings correspond with materials that are "bright red" and "dark gray" at visible wavelengths. "Normal bright soil" exhibits a high albedo, an intermediate 3.0- $\mu\text{m}$  absorption, a relatively strong 2.2- $\mu\text{m}$  absorption, and a flat spectral slope; "normal dark soils" exhibit a strong 2- $\mu\text{m}$  pyroxene absorption and a relatively weak 3.0- $\mu\text{m}$  absorption. Each group can be subdivided further based on position and shape of the ferric iron absorption in bright regions, and in dark regions, spectral slope, strength of the 3.0- $\mu\text{m}$  absorption, and position and shape of the 1- $\mu\text{m}$  and 2- $\mu\text{m}$  absorptions due to Fe in pyroxene. "Transitional" soils, which occur largely at borders of "normal" bright and dark soils, are intermediate to "normal" bright and dark soils in most respects but have a negative spectral slope.